

Structure and thermochemistry of K_2Rb , KRb_2 , and K_2Rb_2

Jason N. Byrd, John A. Montgomery Jr., and Robin Côté

Department of Physics, University of Connecticut, Storrs, Connecticut 06269, USA

(Received 23 March 2010; published 30 July 2010)

The formation and interaction of ultracold polar molecules is a topic of active research. Understanding possible reaction paths and molecular combinations requires accurate studies of the fragment and product energetics. We have calculated accurate gradient optimized ground-state structures and zero-point corrected atomization energies for the trimers and tetramers formed by the reaction of KRb with KRb and corresponding isolated atoms. The K_2Rb and KRb_2 trimers are found to have global minima at the C_{2v} configuration with atomization energies of 6065 and 5931 cm^{-1} while the tetramer is found to have two stable planar structures, of D_{2h} and C_s symmetry, which have atomization energies of 11131 cm^{-1} and 11133 cm^{-1} , respectively. We have calculated the minimum energy reaction path for the reaction $KRb + KRb \rightarrow K_2 + Rb_2$ and found it to be barrierless.

DOI: 10.1103/PhysRevA.82.010502

PACS number(s): 31.15.A–

The formation and interaction of ultracold polar molecules is a topic of great current interest in physics. New techniques for the formation of rovibrational ground-state polar molecules via stimulated rapid adiabatic passage (STIRAP) [1] or Feshbach-optimized photoassociation (FOPA) [2] allow experiments to be performed with $v = 0$ heteronuclear diatomic molecules, including KRb [3–6] and $LiCs$ [7]. Proposals for quantum computation with polar molecules [8,9] have generated a growing need for understanding of the dynamics of diatom-diatom collisions. Such studies of diatomic dynamics require knowledge of the open and closed channels relevant in those reactions. The purpose of the present paper is to present accurate *ab initio* calculations of the structure and thermochemistry of several chemical species relevant to the study of KRb - KRb dimer interactions.

Theoretical work on electronic structure of few-body alkali systems has been limited to lighter homonuclear trimers, in particular, doublet [10] and quartet [11] Li_3 , doublet K_3 [12], and quartet Na_3 [13]. The recent work of Żuchowski and Hutson [14] has characterized the atomization energy of the alkali-metal homo- and heteronuclear triatomic species formed from Li , Na , K , Rb , and Cs . These homonuclear trimers have A' ground electronic states in C_s symmetry that correlate to B_2 symmetry in C_{2v} . Previous mixed alkali tetramer studies have been limited to structure studies of Li_nX_m ($X = Na$ and K) [15,16] and that of $RbCs + RbCs$ [17]. To date no such calculations have been reported for the heteronuclear K_nRb_m tetramer molecules.

Electronic structure calculations were performed on K_2 , Rb_2 , KRb , K_2Rb , KRb_2 , and K_2Rb_2 at the CCSD(T) [18] level of theory. As core-valence effects can be important in alkali metals, we correlate the inner valence electrons in potassium, keeping only $1s^22s^22p^2$ in the core. Rubidium is heavy enough that relativistic effects are significant, so we replace its inner shell electrons by the Stuttgart small-core relativistic (ECP28MDF) effective core potential (ECP) [19]. Basis sets are taken from the Karlsruhe def2-TZVPP [20] and def2-QZVPP [21] orbital and fitting sets.

Optimized geometries for K_2 , Rb_2 , KRb , K_2Rb , KRb_2 , and K_2Rb_2 were found at the CCSD(T)/def2-TZVPP level of theory. Calculation of the harmonic vibrational frequencies was done to verify that the calculated structures were minima

on the potential energy surface, and the calculated frequencies were used to obtain vibrational zero-point energy (ZPE) corrections. These structures were further optimized at the CCSD(T)/def2-QZVPP level of theory, leading to a 0.07-Å correction in the bond lengths and 60 cm^{-1} in final atomization energies. The CCSD(T)/def2-QZVPP geometries are tabulated in Table I.

Evaluation of the contribution of scalar relativistic corrections to K_2 indicate a small 0.005-Å and $<8\text{-}cm^{-1}$ contribution in all electron correlation calculations [24], while for Rb_2 it has been shown [25] that the small core Stuttgart pseudopotential gives an accurate representation of relativistic effects on the bond length and dissociation energy.

Single-point energy calculations were then done using the CCSD(T)-F12b [26,27] [explicitly correlated CCSD(T)] level of theory. The use of explicitly correlated methods accelerate the slow convergence of the one-particle basis set by including terms containing the interelectron coordinates into the wave function [28], thus yielding very accurate results using triple and quadruple zeta basis sets. In addition, we estimate the complete basis set (CBS) limit using the two-point extrapolation formula of Helgaker *et al.* [29],

$$E_{CBS} = \frac{n^3 E_n - (n-1)^3 E_{n-1}}{n^3 - (n-1)^3}. \quad (1)$$

In Table II the CCSD(T) and CCSD(T)-F12b dissociation energies for the def2-TZVPP and def2-QZVPP basis sets are tabulated as well as the zero-point energy corrected atomization energies. After extrapolation, the diatomic CCSD(T)-F12b ZPE corrected dissociation energies agree very well with the experimental diatomic dissociation energies, as shown in Table II. The *ab initio* calculations were done using the GAUSSIAN 09 [30] and MOLPRO [31–33] packages.

We have found that both K_2Rb and KRb_2 have two energetically close local minima on the ground-state surface, one of C_{2v} symmetry and another less symmetric C_s structure (geometries given in Table I). While dependent on the level of theory used to evaluate the atomization energy, we conclude that the symmetric C_{2v} geometry is the global minima for each trimer. The atomization energies calculated are found to be in good agreement with those recently published by Żuchowski and Hutson [14].

TABLE I. Calculated CCSD(T)/QZVPP molecular geometries (in Ångströms and degrees).

r_e				
K ₂	3.956			
Rb ₂	4.233			
KRb	4.160			
	$r_{\text{K-Rb}}$	$r'_{\text{K-Rb}}$	θ	
K ₂ Rb C _{2v}	4.279	4.279	70.68	
K ₂ Rb C _s	4.361	5.234	48.81	
KRb ₂ C _{2v}	4.271	4.271	82.13	
KRb ₂ C _s	4.193	5.179	57.07	
	$r_{\text{Rb-Rb}}$	$r_{\text{K-K}}$	$r_{\text{K-Rb}}$	$\theta_{\text{K-Rb-Rb}}$ $\theta_{\text{K-K-Rb}}$
K ₂ Rb ₂ D _{2h}	8.224	4.0307	4.579	
K ₂ Rb ₂ C _s	4.761	4.408	4.189	53.34 55.48

The K₂Rb₂ tetramer is found to have two nearly degenerate minima on the potential energy surface. One is a rhombic structure of D_{2h} symmetry, and another planar (C_s) structure that corresponds to an interchange of K and Rb atoms. These structures are bound by ~ 3000 cm⁻¹ with respect to K₂ + Rb₂ or KRb + KRb. The electronic structure of these two isomers is very similar, and their stability is likely due to three-center bonds of the sort proposed for Li_nNa_{4-n} clusters [15,16]. The rhombic K₂Rb₂ structure has a short (~ 4 Å) distance and a long (~ 8 Å) Rb-Rb distance. The equivalent structure where the K-K distance is short and the Rb-Rb distance is long is found to be a transition state, not a stable minimum.

To determine if there is any barrier to the KRb + KRb → K₂Rb₂ → Rb₂ + K₂ reaction, we calculate a minimum energy path for the KRb + KRb → K₂Rb₂ and Rb₂ + K₂ → K₂Rb₂ reactions. We start by locating the minimum energy geometric configuration at long range. This is done by calculating *ab initio* the dipole and quadrupole electrostatic moments of K₂, Rb₂, and KRb and then minimizing the long-range electrostatic interaction energy [34] with respect to the angular configuration of the molecules. This minimization resulted in a T-type geometry for both K₂ + Rb₂ and KRb + KRb. We have recently shown that long-range expansions of this type accurately reproduce diatom-diatom interaction energies [35].

TABLE II. Dissociation and zero-point energies calculated using CCSD(T) and CCSD(T)-F12b correlation methods with successive basis sets and CBS extrapolated values (in cm⁻¹).

	ZPE TZVPP	D_e TZVPP		D_e QZVPP		D_0 CBS	
	CCSD(T)	CCSD(T)	CCSD(T)-F12b	CCSD(T)	CCSD(T)-F12b	CCSD(T)	CCSD(T)-F12b
K ₂ ^a	46.0	409 8.8	427 6.9	446 0.0	436 9.7	467 7.6	439 1.5
Rb ₂ ^b	26.8	349 4.3	372 3.3	384 2.7	388 5.4	407 0.2	397 6.8
KRb ^c	35.4	382 9.4	401 5.6	413 5.6	412 8.7	432 3.6	417 5.7
K ₂ Rb C _{2v}	69.8	558 8.2	580 5.5	606 7.7	599 5.7	657 4.2	600 9.4
K ₂ Rb C _s	72.4	560 6.3	584 3.7	617 9.1	601 5.9	652 4.7	606 9.1
KRb ₂ C _{2v}	62.8	539 4.5	563 5.1	591 1.0	584 2.2	604 3.5	578 8.3
KRb ₂ C _s	59.0	521 5.9	547 5.4	572 8.5	569 0.4	622 5.1	593 0.5
K ₂ Rb ₂ D _{2h}	129.5	102 10.8	106 69.4	112 75.3	110 11.1	119 22.7	111 31.0
K ₂ Rb ₂ C _s	126.2	101 98.3	106 29.9	112 11.4	109 93.7	118 24.6	111 33.0

^aExperimental value 4405.389 cm⁻¹ [22].^bExperimental value 3965.8 cm⁻¹ [23].^cExperimental value 4180.417 cm⁻¹ [5].

From these initial geometries, the reaction path was followed by freezing the diatom-diatom distance and optimizing the diatomic bond lengths and angular orientations at the frozen core CCSD(T)/def2-TZVPP level of theory. Single-point energies were evaluated along this path using the CCSD(T)-F12b level of theory including the core-valence correlation energy and extrapolated to the CBS limit as discussed above. This procedure, in which a high-level energy profile is evaluated along a reaction path calculated at a lower level of theory, is known to be a good approximation to the energy profile along the reaction path calculated at the high level of theory [36].

We find that the KRb + KRb dissociation limit connects to the D_{2h} minima while the K₂+Rb₂ dissociation limit connects to the C_s minima, with no barrier found to either reaction. A similar conclusion was obtained for the RbCs + RbCs → Rb₂ + Cs₂ reaction by Tscherbul *et al.* [17]. To finish characterizing the reaction path going from one dissociation limit to the other, we locate the transition state and calculate the intrinsic reaction coordinate (IRC) [37] reaction path connecting the C_s and D_{2h} minima structures at the same level of theory as described previously. Optimizing the transition-state geometry at the inner valence CCSD(T)/def2-TZVPP discussed previously and evaluating an accurate atomization energy using our CCSD(T)-f12b prescription we find that the transition state is 1167.3 cm⁻¹ above the D_{2h} dissociation energy. The calculated reaction path is plotted in Fig. 1 using the approximate reaction coordinate,

$$\Delta R = \frac{1}{2}(R_{\text{K-K}} + R_{\text{Rb-Rb}}) - \frac{1}{2}(R_{\text{K-Rb}} + R'_{\text{K-Rb}}) \quad (2)$$

where $R_{\text{A-B}}$ is the distance between atoms A and B.

The formation and trapping of rovibrational ground-state KRb diatoms with a high phase-space density [5] offers the opportunity to study chemical reactions in the ultracold regime [6]. As seen in Fig. 2, the three-body reaction KRb + Rb → Rb₂ + K is energetically forbidden at ultracold temperatures, leaving the endothermic four-body reaction KRb + KRb → Rb₂ + K₂ as the only pathway to forming Rb₂ within the trap. Measurements of the population of Rb₂ within the trap will then allow direct probing of the exchange reaction

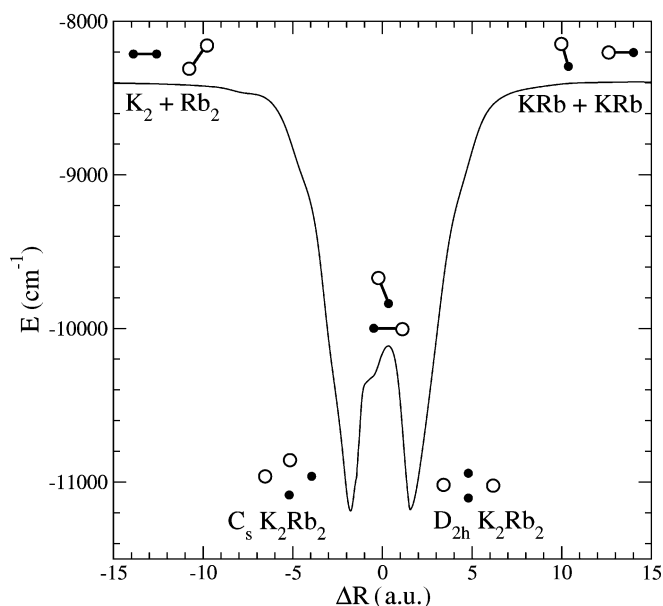


FIG. 1. Minimum energy path connecting the $KRb + KRb$ and $K_2 + Rb_2$ dissociation limits. Included are schematic geometric points of interest, where open and solid circles represent rubidium and potassium atoms, respectively.

rate of $KRb + KRb$. Inherent in this exchange reaction is the possibility of studying the role of fermionic or bosonic spin statistics in ultracold chemical reactions [38–44]. In this temperature regime, s -wave scattering of fermionic ^{40}KRb is suppressed which should greatly diminish the reaction rate of $^{40}KRb + ^{40}KRb$, thus leaving the trap stable to four-body losses. If instead the trap was formed with bosonic ^{39}KRb or ^{41}KRb molecules, no such collisional suppression is expected, where we then expect comparably large reaction rates to occur. It is also possible to explore recent theoretical predictions [44] which show that if a bosonic dimer is composed of two

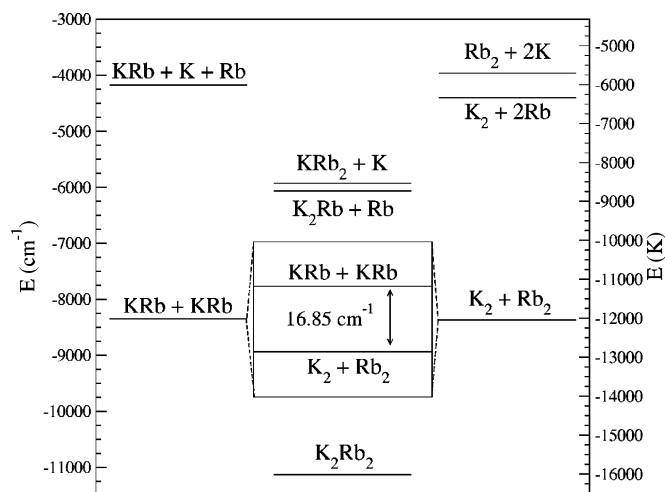


FIG. 2. Schematic energy-level diagram for fragment and structure energies involving KRb with KRb and separated atoms. Inset shows the small difference between the $KRb + KRb$ and $K_2 + Rb_2$ asymptotes.

fermions of very different masses the resulting exchange reaction should still be suppressed despite the overall bosonic nature. This could be accomplished by using fermionic ^{40}K and a long-lived ^{84}Rb or ^{86}Rb . The comparison between reaction rates in the previously described interactions can then be used to directly study the effects of fermion or boson spin statistics to that of chemical reactions.

ACKNOWLEDGMENTS

We thank W. C. Stwalley for helpful discussions during the course of this work. J.N.B. thanks the US Department of Energy Office of Basic Energy Sciences for support and R.C. thanks the Department of Defense Air Force Office of Scientific Research for partial support.

- [1] N. V. Vitanov, M. Fleischhauer, B. W. Shore, and K. Bergmann, *Adv. At. Mol. Phys.* **46**, 55 (2001).
- [2] P. Pellegrini, M. Gacesa, and R. Côté, *Phys. Rev. Lett.* **101**, 053201 (2008).
- [3] J. J. Zirbel, K.-K. Ni, S. Ospelkaus, T. L. Nicholson, M. L. Olsen, P. S. Julienne, C. E. Wieman, J. Ye, and D. S. Jin, *Phys. Rev. A* **78**, 013416 (2008).
- [4] S. Ospelkaus, A. Pe'er, K.-K. Ni, J. J. Zirbel, B. Neyenhuis, S. Kotochigova, P. S. Julienne, J. Ye, and D. S. Jin, *Nature Phys* **4**, 622 (2008).
- [5] K.-K. Ni, S. Ospelkaus, M. H. G. de Miranda, A. Pe'er, B. Neyenhuis, J. J. Zirbel, S. Kotochigova, P. S. Julienne, D. S. Jin, and J. Ye, *Science* **322**, 231 (2008).
- [6] S. Ospelkaus, K.-K. Ni, D. Wang, M. H. G. de Miranda, B. Neyenhuis, G. Quemener, P. S. Julienne, J. L. Bohn, D. S. Jin, and J. Ye, *Science* **327**, 853 (2010).
- [7] J. Deiglmayr, A. Grochola, M. Repp, K. Mörtlbauer, C. Glück, J. Lange, O. Dulieu, R. Wester, and M. Weidemüller, *Phys. Rev. Lett.* **101**, 133004 (2008).
- [8] S. F. Yelin, K. Kirby, and R. Côté, *Phys. Rev. A* **74**, 050301(R) (2006).
- [9] E. Kuznetsova, R. Côté, K. Kirby, and S. F. Yelin, *Phys. Rev. A* **78**, 012313 (2008).
- [10] J. N. Byrd, J. A. Montgomery Jr., H. H. Michels, and R. Côté, *Int. J. Quantum Chem.* **109**, 3112 (2009).
- [11] M. T. Cvitaš, P. Soldán, J. Hutson, P. Honvault, and J.-M. Launay, *J. Chem. Phys.* **127**, 074302 (2007).
- [12] A. Hauser, C. Callegari, P. Soldán, and W. Ernst, *J. Chem. Phys.* **129**, 044307 (2008).
- [13] A. Simoni, J.-M. Launay, and P. Soldán, *Phys. Rev. A* **79**, 032701 (2009).
- [14] P. S. Żuchowski and J. M. Hutson, *Phys. Rev. A* **81**, 060703 (2010).
- [15] T. A. Dahlseid, M. M. Kappes, J. A. Pople, and M. A. Ratner, *J. Chem. Phys.* **96**, 4924 (1992).
- [16] Z.-Y. Jiang, K.-H. Lee, S.-T. Li, and S.-Y. Chu, *Int. J. Mass. Spectrom* **253**, 104 (2006).

- [17] T. V. Tscherbul, G. Barinovs, J. Kłos, and R. V. Krems, *Phys. Rev. A* **78**, 022705 (2008).
- [18] G. D. Purvis III and R. J. Bartlett, *J. Chem. Phys.* **76**, 1910 (1982).
- [19] I. Lim, P. Schwerdtfeger, B. Metz, and H. Stoll, *J. Chem. Phys.* **122**, 104103 (2005).
- [20] F. Weigend and R. Ahlrichs, *Phys. Chem. Chem. Phys.* **7**, 3297 (2005).
- [21] F. Weigend, F. Furche, and R. Ahlrichs, *J. Chem. Phys.* **119**, 12753 (2003).
- [22] S. Falke, I. Sherstov, E. Teimann, and C. Lisdat, *J. Chem. Phys.* **125**, 224303 (2006).
- [23] C. Amiot, *J. Chem. Phys.* **93**, 8591 (1990).
- [24] M. A. Iron, M. Oren, and J. M. Martin, *Mol. Phys.* **101**, 1345 (2003).
- [25] I. Lim, P. Schwerdtfeger, T. Söhnle, and H. Stoll, *J. Chem. Phys.* **122**, 134307 (2005).
- [26] T. B. Adler, G. Knizia, and H.-J. Werner, *J. Chem. Phys.* **127**, 221106 (2007).
- [27] G. Knizia, T. B. Adler, and H.-J. Werner, *J. Chem. Phys.* **130**, 054104 (2009).
- [28] T. Helgaker, W. Klopper, and D. P. Tew, *Mol. Phys.* **106**, 2107 (2008).
- [29] T. Helgaker, W. Klopper, H. Koch, and J. Noga, *J. Chem. Phys.* **106**, 9639 (1997).
- [30] M. J. Frisch, G. W. Trucks, H. B. Schlegel, G. E. Scuseria *et al.*, computer code GAUSSIAN 09, Revision A.2, Gaussian, Wallingford, CT, 2009.
- [31] H.-J. Werner, P. J. Knowles, R. Lindh, F. R. Manby, M. Schütz *et al.*, computer code MOLPRO, Version 2009.1, Cardiff University, Cardiff, UK, 2009.
- [32] C. Hampel, K. Peterson, and H.-J. Werner, *Chem. Phys. Lett.* **190**, 1 (1992).
- [33] P. J. Knowles, C. Hampel, and H.-J. Werner, *J. Chem. Phys.* **99**, 5219 (1993).
- [34] A. J. Stone, *Theory of Intermolecular Forces* (Oxford University Press, Oxford, 1996).
- [35] W. T. Zemke, J. N. Byrd, H. H. Michels, J. A. Montgomery Jr., and W. C. Stwalley, *J. Chem. Phys.* **132**, 244305 (2010).
- [36] D. K. Malick, G. A. Petersson, and J. A. Montgomery Jr., *J. Chem. Phys.* **108**, 5704 (1998).
- [37] K. Fukui, *Acc. Chem. Res.* **14**, 363 (1981).
- [38] M. T. Cvitaš, P. Soldaň, J. M. Hutson, P. Honvault, and J. M. Launay, *Phys. Rev. Lett.* **94**, 200402 (2005).
- [39] M. T. Cvitaš, P. Soldaň, J. M. Hutson, P. Honvault, and J. M. Launay, *Phys. Rev. Lett.* **94**, 033201 (2005).
- [40] J. P. D’Incao, B. D. Esry, and C. H. Greene, *Phys. Rev. A* **77**, 052709 (2008).
- [41] J. P. D’Incao, S. T. Rittenhouse, N. P. Mehta, and C. H. Greene, *Phys. Rev. A* **79**, 030501(R) (2009).
- [42] D. S. Petrov, C. Salomon, and G. V. Shlyapnikov, *Phys. Rev. A* **71**, 012708 (2005).
- [43] E. R. Hudson, N. B. Gilfooy, S. Kotochigova, J. M. Sage, and D. DeMille, *Phys. Rev. Lett.* **100**, 203201 (2008).
- [44] B. Marcelis, S. J. J. M. F. Kokkelmans, G. V. Shlyapnikov, and D. S. Petrov, *Phys. Rev. A* **77**, 032707 (2008).